Effects of Downstream Plasma Exposure on β-Ga_2O_3 Rectifiers

Xinyi Xia[1], Minghan Xian[1], Chaker Fares[1], Fan Ren[1], Junghun Kim[2], Jihyun Kim[2], Marko Tadjer[3] and Stephen J. Pearton[4]

[1]Department of Chemical Engineering, University of Florida, Gainesville, Florida 32608, USA

[2]Department of Chemical and Biological Engineering, Korea University, Seoul 02841, Republic of Korea

[3]U.S. Naval Research Laboratory, 4555 Overlook Ave SW, Washington, DC 20375, USA

[4]Department of Materials Science and Engineering, University of Florida, Gainesville, Florida 32608, USA

Abstract

The effects of downstream plasma exposure with O_2, N_2 or CF_4 discharges on Si-doped Ga_2O_3 Schottky diode forward and reverse current-voltage characteristics were investigated. The samples were exposed to discharges with rf power of 50 W plasma at a pressure of 400 mTorr and a fixed treatment time of 1 min to simulate dielectric layer removal, photoresist ashing or surface cleaning steps. Schottky contacts were deposited through a shadow mask after exposure to avoid any changes to the surface. A Schottky barrier height of 1.1 eV was obtained for the reference sample without plasma treatment, with an ideality factor of 1.0. The diodes exposed to CF_4 showed a 0.25V shift from the I-V of the reference sample due to a Schottky barrier height lowering around 14 %. The diodes showed a decrease of Schottky barrier height of 2.5 and 6.5 % with O_2 or N_2 treatments, respectively. The effect of plasma exposure on the ideality factor of diodes treated with these plasmas was minimal; 0.2% for O_2 and N_2, 0.3% for CF_4, respectively. The reverse leakage currents were 1.2, 2.2 and 4.8 μA/cm^2 for the diodes treated with O_2, and CF_4, and N_2 respectively. The effect of downstream plasma treatment on diode on-resistance and

on-off ratio were also minimal. The changes observed are much less than caused by exposure to hydrogen-containing plasmas and indicate that downstream plasma stripping of films from Ga_2O_3 during device processing is a relatively benign approach.

Introduction

The ultra-wide bandgap semiconductor β-Ga_2O_3 has attracted increasing attention because of the prospects for use in next generation high-power electronics [1-4]. The high breakdown field of this material has enabled numerous demonstrations of vertical rectifiers with breakdown voltages in the kV range [5-22]. This is of interest for electric vehicle (EV) charging stations, power management in residential solar systems and battery energy storage systems. This high breakdown field of Ga_2O_3 enables greater voltage blocking capability and lower conduction losses due to a lower on-resistance reduction in comparison with Si-based devices [1-4].

One important factor that needs to be considered when forming devices using β- Ga_2O_3 is the electronic behavior at the surface or interfaces. The surface termination, relaxation and surface energies for different faces of β-Ga_2O_3 have been reported by Bermudez [23]. However, it is not widely appreciated that the surface of β-Ga_2O_3 can be strongly affected by exposure to gaseous or plasma environments and the influence of changing conductivity and roles of surface states in oxidizing or reducing environments are not well-established [24-37]. This is despite the fact that Ga_2O_3 rectifiers are known to be sensitive detectors of hydrogen [25,26]. The (-201) Ga_2O_3 surface has been reported to be particularly sensitive to plasma-induced damage, leading to device performance degradation [33].

In our study, we have employed truly downstream plasma exposures of Ga_2O_3 to CF_4, N_2 and O_2 to separate out chemical effects from physical damage due to ion bombardment and also to simulate processes like photoresist ashing, dielectric removal and surface cleaning that occur during device fabrication [29,34]. We find that only CF_4 exposure leads to significant changes under these conditions. This work complements previous studies where the Ga_2O_3 was exposed

to these plasmas in immersive mode, where combined chemical and physical bombardment effects are present [24,28,29].

Experimental

The starting samples consisted of vertical rectifier structures. The drift region of the material consisted of a 10 μm thick, lightly Si doped epitaxial layer grown by halide vapor phase epitaxy (HVPE) with carrier concentration of $3x10^{16}$ cm^{-3}, and this epitaxial layer was grown on a (001) surface orientation Sn-doped ($n=10^{19}$ cm^{-3}) β-Ga_2O_3 single crystal (Novel Crystal Technology, Japan). The wafer surfaces were ultrasonically cleaned in acetone, methanol, and isopropyl alcohol prior to all experiments. The Fermi level is found to be relatively unpinned on the bulk β-Ga_2O_3 (001) substrate, suggesting the presence of lower density of oxygen vacancy states on its surface [37].

A full area Ti/Au backside Ohmic contact was formed by e-beam evaporation and was annealed at 550 ̊C for 30s under N_2 ambient. After backside Ohmic formation, the front of the sample was cleaned using HCl and then treated with ozone for 20 minutes to remove residual hydrocarbons. Previous reports have indicated that untreated substrates contain a significant amount of adsorbed carbon contaminations at the surface, which can be partly removed by annealing at 800◦C in UHV. In that uncleaned state, upward band bending of about 0.5 eV that increases with annealing is present, leading to an electron depletion layer at the near-surface region [27]. This effect could be removed either by annealing in oxygen at high temperatures or by chemical cleaning /etching of the surface prior to deposition of metal contacts [27].

The plasma treatments were performed using a downstream PIE Scientific Tergeo Plasma Cleaner with O_2, N_2 or CF_4 discharges. The plasma was generated with a 13.56MHz high frequency rf power supply with automatic impedance matching for the in-situ plasma source.

The RF power source could operate over the range 0-150 watt, and in our case we used 50W to generate the plasma at a pressure of 400 mTorr, with a fixed treatment time of 1 min. The system can be operated either in immersion mode (samples are immersed in plasma) or downstream mode (samples are placed outside the plasma) and we used the latter in all cases. In the downstream mode, there is no physical bombardment of the sample surface by energetic ions that would occur in the immersion mode. However, there can still be chemically-induced changes to the near-surface in the downstream mode that affect properties such as Schottky barrier height. In addition to the ion bombardment effects in the immersion mode, there can be synergistic effects due to the combined ion and reactive neutral components. This is absent in the downstream mode.

Next, the front of the samples was treated with ozone for 15 min, followed by cleaning with 1:10 diluted HCl, then was treated with ozone for another 15 minutes to remove surface contamination. the Schottky contacts were formed by e-beam evaporation. Ni/Au Schottky metallization was deposited through a shadow metal rather than photoresist patterning to avoid changing the chemistry of the Ga_2O_3 surface. Edge termination was not used, also in order to focus on the surface characteristics free of any edge effects [9]. The completed devices had circular contact diameters of 800 μm.

The current-voltage (I-V) characteristics were recorded at room temperature. Forward and reverse current measurements were recorded with a HP 4156 parameter analyzer. The forward direction was dominated by the thermionic emission (TE) current over most of the temperature range, while in the reverse direction, the thermionic field emission (TFE) and tunneling currents played an important role at high reverse bias. To extract the zero-bias equivalent barrier height (Φ_b) and ideality factor (n), we used the relationship for current density in TE theory and the

linear portion of the forward bias characteristics through the correction factor $[eE/4\pi\varepsilon]^{0.5}$, where E is the electric field at the Ni/Au/Ga_2O_3 interface and ε is the dielectric constant of the semiconductor [37], ie. $J = J_0 \exp(eV_A/nkT)[1-\exp(-eV_A/kT)$ where $J_0 = A^* m_{eff}/m_0 T^2 \exp(\Phi_B/kT)$, e is electronic charge and A^* is the Richardson constant (33.7 $A.cm^{-2}K^{-2}$) and V_A is the bias voltage applied. The values of barrier height were corrected for the image force (IF) lowering, as described elsewhere [38]. Capacitance-Voltage (C-V) characteristics were recorded with an Agilent 4284A Precision LCR Meter to conform the carrier concentration in the epi layer.

The forward turn-on voltage, V_F, for a Schottky rectifier is given by

$$V_F = \frac{nkT}{e} ln(\frac{J_F}{A^{**}T^2}) + n\Phi_B + R_{ON} \cdot J_F$$

where R_{ON} is the on-state resistance. We defined V_F as the bias at which the forward current density is 100 $A \cdot cm^{-2}$.The diode on/off ratio is another figure-of-merit and was measured when switching from 1V forward to reverse biases up to 100V.

Results and Discussion

The I-V results before and after downstream plasma exposure are shown in Figure 1 on both log (a) and linear (b) scales. Near-ideal Schottky characteristics with n values of 1.0 were obtained for the reference diodes, with a barrier height of 1.1 eV. We used I-V data rather than capacitance -voltage data because nonlinear doping profiles can affect the latter. From the forward I-V characteristic, as illustrated in Figure 1, the diodes exposed to CF_4 showed a 0.25V shift from the I-V of the reference sample due to a Schottky barrier height lowering around 14 %, as shown in Table 1. This can result from the change in barrier height from the relation above for V_F. Previous work has shown that under partially immersive CF_4 plasma exposure conditions, high concentrations of fluorine are incorporated into the near-surface region of Ga_2O_3 and that it

remains in the material to temperatures beyond 400 ℃ [24]. It is clear that compensation of Si donors by F^- ions occurs in Ga_2O_3, leading to changes in effective barrier height [24].

The diodes exposed to downstream N_2 and O_2 plasmas showed small decreases of Schottky barrier height of 2.5 and 6.5 % with O_2 or N_2 treatments, respectively, as shown in Figure 2. It has been previously reported that Ga_2O_3 displays electron accumulation when the surface is terminated by O -H groups [27], resulting in downward band bending. After removal of the hydrogen by surface cleaning, the direction of this band bending is reversed and the surface displays electron depletion. This has been explained by the charge neutrality level, which is found to be 0.6 eV below the conduction band minimum [27]. This is supported by the determination of the charge state transition level for *H* interstitials, which do not disrupt the bonding on the Ga_2O_3 surface, but are captured by O lone-pairs on the surface, forming shallow donors [27,36,39,40]. However, in our case, it is clear that the surface is sufficiently stable after downstream plasma exposures to O_2 that subsequent exposure to air does not change the barrier height to the level exhibited by O-H bonding. The effect of plasma exposure on the ideality factor of diodes treated with these plasmas was minimal; 0.2% for O_2 and N_2, 0.3% for CF_4, respectively, as also shown in Figure 2.

The incorporation of F- in Ga_2O_3 under immersive plasma conditions was previously found to lead to an increase of the barrier height [28]. However, in this current work with remote plasmas, the data shows a small decrease of the barrier height. Thus it is clear that the incorporation of F is assisted by the ion bombardment present in immersive plasmas. This is plausible given the need for the F to diffuse enough to produce the compensation effect of Si donors by F- ions. The ion bombardment can produce enough near-surface point defects to assist

this diffusion .In the case of downstream plasma, the F compensation effect is absent and the changes are due to subtle near-surface changes in the chemistry of the upper layers

The reverse leakage currents were 1.2, 2.2 and 4.8 μA/cm^2 for the diodes treated with O_2, and CF_4, and N_2 respectively, as shown in Figure 3. The respective reverse breakdown voltages (V_B) are shown in Table 1, with only minor changes as a result of the downstream plasma exposure. As expected, this indicates that the number of midgap states leading to recombination or tunneling currents is not significantly changed as a result of the downstream plasma exposure or else we would observe increases in the reverse current density. The absence of ion bombardment is clearly the main factor. Notice also in Table 1 that the surface roughness as measured by Atomic Force Microscopy (AFM) over an area of 5 x 5 μm^2, did not show any significant change. The near-surface Ga/O ratio averaged over a depth of ~100Å by X-Ray Photoelectron Spectroscopy did not change, as expected. It would be difficult to correlate these measurements to the change in electrical properties, since the latter are dominated by the first few layers of the surface.

The effects of downstream plasma treatment on diode on-resistance were also minimal as shown in Figure 4, where the increases are <10% for all the different plasma chemistries. Since

$$R_{diode} = R_{drift} + R_{sub} + R_{contact}$$

where specific on-state resistance of a unipolar diode is a sum of the drift region resistance R_{drfit}, the contact resistance $R_{contact}$ and the substrate resistance. R_{sub} [1], this means that the latter hasn't changed much during exposure to the fluorine, oxygen or nitrogen- based discharges. A similar conclusion can be drawn from the diode on/off ratio data in Figure 5, where the changes are small (<10 %). The on-off ratio is another figure of merit in that having high on-current and

low leakage current in reverse bias is desirable. This was $>10^5$ for all devices measure, independent of plasma exposure.

Finally, to give some idea of variability across samples, the range of barrier heights and ideality factors measured from 6 different devices on each chip are shown in Figure 6. Within the experimental error, only samples exposed to CF_4 show significant changes in these two parameters.

The crystal structure of β Ga_2O_3 consists of double octahedral chains, running parallel to the crystallographic y-axis [41]. The chains are cross-linked by tetrahedral GaO_4 groups. Figure 7 shows the crystal structure for the (001) orientation used here [37], where the surface consists mostly of oxygen termination. In terms of intrinsic defects in n-type Ga_2O_3, the reported high formation energy of oxygen vacancies (V_O) suggests they are deep donors that are not ionized in n-type material and this will not contribute to the conductivity [28,36]. The Ga vacancy (V_{Ga}) is expected to be a triple acceptor, while the oxygen interstitial (Oi) is neutral, and the gallium interstitial (Gai) are in the 3+ charge state. [28,36] The V_{Ga} concentration increases with oxygen partial pressure, leading to a conductivity compensation. What is clear from our data is that this O-terminated surface is stable against air and O_2 exposure, but there are small changes with fluorine exposure that are smaller than in the case of performing the CF_4 exposure in an immersive plasma environment. The ion bombardment in that case enhance the chemical effects of the fluorine.

Summary and Conclusions

There are numerous cases during Ga_2O_3 device fabrication where plasmas are used in resist stripping, surface cleaning or dielectric layer removal. Our results show that purely downstream plasmas produce only small changes in surface properties. There are still some unanswered

questions as to what effect the crystal orientation has, since the surface termination is different in different crystal directions and it is known that the bulk properties of Ga_2O_3 are highly anisotropic. Similarly, what is the effect of polytype, since the α polytype is promising due to its even larger bandgap than for β Ga_2O_3. Lastly, what effect will alloying with Al and In have when those $(Al_xGa_{1-x})_2O_3$ and $(In_xGa_{1-x})_2O_3$ alloys are used in device structures? It would be expected that the Al-based alloys will be more sensitive to both oxygen and fluorine adsorption effects.

Data Availability Statement

All data that support the findings of this study are included within the article (and any supplementary files)

Acknowledgments

The work at UF was performed as part of Interaction of Ionizing Radiation with Matter University Research Alliance (IIRM-URA), sponsored by the Department of the Defense, Defense Threat Reduction Agency under award HDTRA1-20-2-0002. The content of the information does not necessarily reflect the position or the policy of the federal government, and no official endorsement should be inferred. The work at UF was also supported by NSF DMR 1856662 (James Edgar). The work at Korea University was supported by the National Research Foundation (NRF) of Korea (2020M3H4A3081799). The work at NRL was supported by the Office of Naval Research.

References

[1] S. J. Pearton, F. Ren, M. Tadjer and J. Kim, Perspective: Ga_2O_3 for ultra-high power rectifiers and MOSFETS, J. Appl. Phys., 124, 220901 (2018).

[2] E. Ahmadi and Y. Oshima, Materials issues and devices of α- and β-Ga_2O_3, J. Appl. Phys. 126 (16), 160901 (2019)

[3] S. J. Pearton, J. Yang, P. H. Cary, F. Ren, J. Kim, M. J. Tadjer, and M.A. Mastro, A review of Ga_2O_3 materials, processing, and devices, Appl. Phys. Rev., 5, 011301 (2018).

[4] M.H. Wong and M. Higashiwaki, Vertical β-Ga_2O_3 Power Transistors: A Review, IEEE Trans. Electron Dev. 67, 3925 (2021).

[5] N. Allen, Ming Xiao, Xiaodong Yan, Kohei Sasaki, Marko J. Tadjer, Jiahui Ma, Ruizhe Zhang, Han Wang and Yuhao Zhang, Vertical Ga_2O_3 Schottky Barrier Diodes with Small-Angle Beveled Field Plates: A Baliga's Figure-of-Merit of 0.6 GW/cm^2,I EEE Electron Dev. Lett., 40, 1399 (2019).

[6] K. Konishi, K. Goto, H. Murakami, Y. Kumagai, A. Kuramata, S. Yamakoshi, and M. Higashiwaki, 1-kV vertical Ga_2O_3 field-plated Schottky barrier diodes, Appl. Phys. Lett. 110, 103506 (2017).

[7] W. Li, K. Nomoto, Z. Hu, D. Jena, and H. G. Xing, Field-Plated Ga_2O_3 Trench Schottky Barrier Diodes with a BV^2/ Ron of up to 0.95 GW/cm^2,IEEE Electron Dev. Lett., 41, 107 (2020).

[8] M. Ji, Neil R. Taylo, Ivan Kravchenko, Pooran Joshi, Tolga Aytug, Lei R. Cao, M. Parans Paranthaman, Demonstration of Large-Size Vertical Ga_2O_3 Schottky Barrier Diodes, IEEE Trans. Power Electron., 36, 41 (2021).

[9] J.C. Yang, F. Ren, M.J. Tadjer, S.J. Pearton and A. Kuramata, 2300V reverse breakdown voltage Ga_2O_3 Schottky rectifiers, ECS J. Solid State Sci. Technol., 7, Q92 (2018).

[10] Jiancheng Yang, Fan Ren, YenTing Chen, Yu Te Liao, Chin Wei Chang, Jenshan Lin, Marko J. Tadjer, S. J. Pearton and Akito Kuramata, Dynamic Switching Characteristics of 1 A Forward Current Ga_2O_3 Rectifiers, J. Electron. Dev. Soc. 7, 57 (2019).

[11] Z. Hu, Yuanjie Lv, Chunyong Zhao, Qian Feng Zhaoqing Feng, Kui Dang, Xusheng Tian, Yachao Zhang, Jing Ning, Hong Zhou, Xuanwu Kang, Jincheng Zhang and Yue Hao, Beveled fluoride plasma treatment for vertical β-Ga_2O_3 Schottky barrier diode with high reverse blocking voltage and low turn on voltage, IEEE Electron Dev. Lett., 4 441 (2020).

[12] J. Yang, Minghan Xian, Patrick Carey, Chaker Fares, Jessica Partain, Fan Ren, Marko Tadjer, Elaf Anber, Dan Foley, Andrew Lang, James Hart, James Nathaniel, Mitra L Taheri, SJ Pearton, Akito Kuramata, Vertical geometry 33.2 A, 4.8 MW cm^2 Ga_2O_3 field-plated Schottky rectifier arrays, Appl. Phys. Lett., 114, 232106 (2019).

[13] Hongpeng Zhang, Lei Yuan , Xiaoyan Tang, Jichao Hu, Jianwu Sun, Yimen Zhang, Yuming Zhang and Renxu Jia, Progress of ultra-wide bandgap Ga_2O_3 semiconductor materials in power MOSFETs, IEEE Trans Power Electronics 35, 5157 (2020).

[14] Ming Xiao, Boyan Wang, Jingcun Liu, Ruizhe Zhang, Student Zichen Zhang, Chao Ding, Shengchang Lu, Kohei Sasaki, Guo-Quan Lu, Cyril Buttay, and Yuhao Zhang, Packaged Ga_2O_3 Schottky Rectifiers with Over 60 A Surge Current Capability, IEEE Power Electron. Lett (2021).

[15] Yuanjie Lv, Yuangang Wang, Xingchang Fu, Shaobo Dun, Zhaofeng Sun, Hongyu Liu, Xingye Zhou, Xubo Song, Kui Dang, Shixiong Liang, Jincheng Zhang, Hong Zhou, Zhihong Feng, Shujun Cai, and Yue Hao, Demonstration of β-Ga_2O_3 Junction Barrier Schottky Diodes with a Baliga's Figure of Merit of 0.85 GW/cm^2 or a 5A/700 V Handling Capabilities, IEEE Trans. Power Electron. (2020).

[16] H.H. Gong, X. H. Chen, Y. Xu, F.-F. Ren, S. L. Gu, and J. D. Ye, A 1.86-kV double-layered NiO/β-Ga_2O_3 vertical p–n heterojunction diode, Appl. Phys. Lett. 117, 022104 (2020).

[17] Ribhu Sharma, Minghan Xian, Chaker Fares, Mark E. Law, Marko Tadjer, Karl D. Hobart, Fan Ren and S. J. Pearton, Effect of probe geometry during measurement of >100 A Ga_2O_3 vertical rectifiers, J. Vac. Sci. Technol. A 39, 013406 (2021).

[18] Wenshen Li, Kazuki Nomoto, Debdeep Jena and Huili Grace Xing, Thermionic emission or tunneling? The universal transition electric field for ideal Schottky reverse leakage current: A case study in β-Ga_2O_3, Appl. Phys. Lett. 117, 222104 (2020).

[19] W. Xiong, Xuanze Zhou, Guangwei Xu, Qiming He, Guangzhong Jian, Chen Chen, Yangtong Yu, Weibing Hao, Xueqiang Xiang, Xiaolong Zhao, Wenxiang Mu, Zhitai Jia, Xutang Tao and Shibing Long, Double-Barrier β-Ga_2O_3 Schottky Barrier Diode With Low Turn-on Voltage and Leakage Current, IEEE Electron Dev. Lett 42, 430 (2021).

[20] Qinglong Yan, Hehe Gong, Jincheng Zhang, Jiandong Ye Hong Zhou, Zhihong Liu, Shengrui Xu, Chenlu Wang, Zhuangzhuang Hu, Qian Feng, Jing Ning, Chunfu Zhang, Peijun Ma, Rong Zhang and Yue Hao, β-Ga_2O_3 hetero-junction barrier Schottky diode with reverse leakage current modulation and BV^2 /Ron,sp value of 0.93 GW/cm^2, Appl. Phys. Lett. 118, 122102 (2021).

[21] Device Topological Thermal Management of β-Ga_2O_3 Schottky Barrier Diodes, Yang-Tong Yu, Xue-Qiang Xiang, Xuan-Ze Zhou, Kai Zhou, Guang-Wei Xu, Xiao-Long Zhao and Shi-Bing Long, Chinese Physics B, in press https://doi.org/10.1088/1674-1056/abeee2

[22] Weibing Hao, Qiming He, Kai Zhou, Guangwei Xu, Wenhao Xiong, Xuanze Zhou, Guangzhong Jian, Chen Chen, Xiaolong Zhao and Shibing Long, Low defect density and small

I−V curve hysteresis in NiO/β-Ga_2O_3 pn diode with a high PFOM of 0.65 GW/cm2, Appl. Phys. Lett. 118, 043501 (2021).

[23] V. M. Bermudez, The Structure of Low-Index Surfaces of β-Ga_2O_3, Chem. Phys., 2006, 323, 193 (2006).

[24] Jiancheng Yang, Zachary Sparks, Fan Ren, Stephen J. Pearton, and Marko Tadjer, Effect of surface treatments on electrical properties of β-Ga_2O_3, J. Vac. Sci. Technol. **B36**, 061201 (2018).

[25] S. Nakagomi, T. Sai and Y. Kokubun, Hydrogen gas sensor with self-temperature compensation based on β-Ga_2O_3 thin film, Sens. Actuators, B,187, 413 (2013),

[26] Soohwan Jang, Sunwoo Jung, Jihyun Kim, Fan Ren and S. J. Pearton, Hydrogen sensing characteristics of Pt Schottky diodes on (201) and (010) Ga_2O_3 single crystals, ECS J. Solid State Sci. Technol. 7, Q3180 (2018).

[27] J.E.N. Swallow, J.B. Varley, L.A.H. Jones, J. T. Gibbon, L.F.J .Piper, V.R. Dhank and T.D. Veal, Transition from electron accumulation to depletion at β-Ga_2O_3 surfaces: The role of hydrogen and the charge neutrality level. APL Materials 7, 022528 (2019)

[28] Jiancheng Yang, Chaker Fares, F. Ren, Ribhu Sharma, Erin Patrick, Mark E. Law, S.J. Pearton and Akito Kuramata, Effects of Fluorine Incorporation into β Ga_2O_3, J. Appl. Phys. 123, 165706 (2018).

[29] Fan Ren, J.C. Yang, C .Fares and S.J. Pearton, Device Processing and Junction Formation Needs for Ultra High Power Ga_2O_3 Electronics MRS Communications 9,77 (2019).

[30] A.Y. Polyakov, InHwan Lee, N.B. Smirnov, E.B. Yakimov, I.V. Shchemerov, A.V. Chernykh, A.I. Kochkova, A.A. Vasilev, P. H. Carey, F. Ren, David J. Smith and S.J. Pearton,

Defects at the Surface of β Ga_2O_3 Produced by Ar Plasma Exposure, APL Mater.7, 061102 (2019).

[31] A.Y. Polyakov, In Hwan Lee, N.B. Smirnov, E.B. Yakimov, I.V. Shchemerov, A.V. Chernykh, A.I. Kochkova, A.A. Vasilev, F. Ren, P.H. Carey IV and S.J. Pearton, Hydrogen plasma treatment of β Ga_2O_3: changes in electrical properties and deep trap spectra, Appl.Phys. Lett. 115, 032101 (2019).

[32] A.Y. Polyakov, In Hwan Lee, N.B. Smirnov, E.B. Yakimov, I.V. Shchemerov, A.V. Chernykh, A.I. Kochkova, A.A. Vasilev, A.S. Shiko, Patrick H. Carey IV , F. Ren and S.J. Pearton, Effects of hydrogen plasma treatment condition on electrical properties of β Ga_2O_3, ECS J. Solid State Sci. Technol.8, P661 (2019).

[33] A.Y. Polyakov, In- Hwan Lee, Andrew Miakonkikh, A.V. Chernykh, N.B. Smirnov, I.V. Shchemerov, A.I. Kochkova, A.A. Vasilev and S.J. Pearton, Anisotropy of Hydrogen Plasma Effects in Bulk n Type β Ga_2O_3, J. Appl. Phys.127, 175702 (2020).

[34] Jihyun Kim, F. Ren and S.J. Pearton, Will Surface Effects Dominate in Quasi Two Dimensional Gallium Oxide for Electronic and Photonic Devices?, Nanoscale Horizons 4, 1251 (2019).

[35] L. Vines, C. Bhoodoo, H. von Wenckstern and M. Grundmann, Electrical conductivity of In_2O_3 and Ga_2O_3 after low temperature ion irradiation; implications for intrinsic defect formation and charge neutrality level, J. Phys.: Condens. Matter, 30, 025502 (2018).

[36] P. Deak, Q. D. Ho, F. Seemann, B. Aradi, M. Lorke and T. Frauenheim, Choosing the correct hybrid for defect calculations: A case study on intrinsic carrier trapping in β-Ga_2O_3, Phys. Rev. B., 2017, 95, 075208 92017).

[37] Luke A. M. Lyle, Kunyao Jiang, Elizabeth V. Favela, Kalyan Das, Andreas Popp, Zbigniew Galazka, Guenter Wagner, and Lisa M. Porter, Effect of metal contacts on (100) β-Ga_2O_3 Schottky barriers, J. Vac. Sci. Technol. A39, 033202 (2021).

[38] Caixia Hou, Rodrigo M. Gazoni, Roger J. Reeves and Martin W. Allen, Dramatic Improvement in the Rectifying Properties of Pd Schottky Contacts on β-Ga_2O_3 During Their High-Temperature Operation, IEEE Trans Electron Dev, 68, 1791 (2021).

[39] R. Lingaparthi, Q. T. Thieu, K. Koshi, D. Wakimoto, K. Sasaki, and A. Kuramata, Surface states on (001) oriented β-Ga_2O_3 epilayers, their origin, and their effect on the electrical properties of Schottky barrier diodes Appl. Phys. Lett. 116, 092101 (2020).

[40], A. Navarro-Quezada, Z. Galazka, S. Alaméa, D. Skuridina, P. Vogt and N. Essera, Surface properties of annealed semiconducting β-Ga_2O_3 (1 0 0) single crystals for epitaxy, Appl. Surf. Sci. 349, 368 (2015).

[41] M.A. Mastro, C.R. Eddy Jr., M.J. Tadjer, J.K. Hite, J. Kim and S.J. Pearton, Assessment of the Crystal Structure and (010) Surface of β Ga_2O_3 , J. Vac. Sci. Technol A 39, 013408 (2020).

[42] CrystalMaker Software Ltd., http://crystalmaker.com/

Table 1. Summary of diode characteristics as a function of plasma treatments.

	Schottky barrier height (eV)	Ideality factor	R_{ON} ($m\Omega.cm^2$)	V_B (V)	AFM FWHM (nm)	Ga/O ratio
Reference	1.1	1.00	28.6	135	3.5	0.40
N_2 plasma	1.04	1.02	29.6	105	3.5	0.40
O_2 plasma	1.08	1.01	29.1	130	3.6	0.40
CF_4 plasma	0.96	1.04	30.5	105	3.5	0.42

Figure Captions

Figure 1. Forward I-V characteristic from -1 to 1V for samples exposed to different plasmas shown in (a) log or (b) linear scale.

Figure 2. Percentage change of Schottky barrier height and ideality factor for the Ga_2O_3 diodes exposed to O_2, N_2 or CF_4 plasma.

Figure 3. Reverse I-V characteristic from 0 to -100V for samples exposed to different plasmas.

Figure 4. On-resistance for samples exposed to different plasmas

Figure 5. On/off ratio for samples exposed to different plasmas

Figure 6. Schottky barrier height and ideality factor after different plasma treatments plotted as the mean of 6 different measurements (n=6).

Figure 7. Schematic of β Ga_2O_3 crystal structure with the (001) direction being vertical to the top surface [37].

(a)

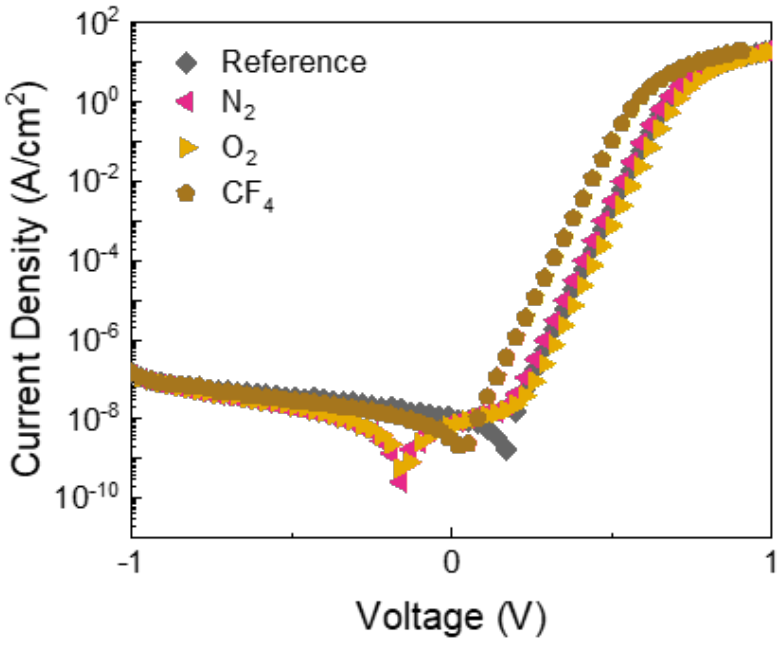
Reference
N2
O2
CF4
Current Density (A/cm2)
10^2
10^0
10^-2
10^-4
10^-6
10^-8
10^-10
-1
0
1
Voltage (V)

(b)

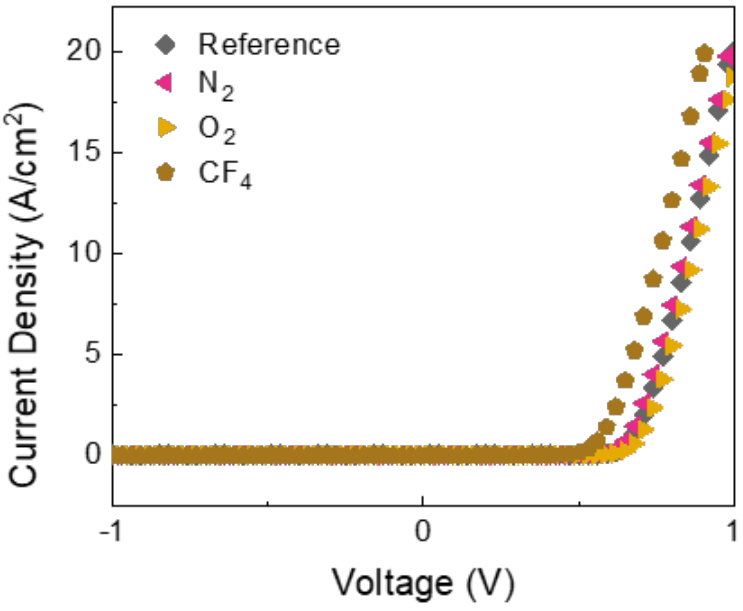
Reference
N2
O2
CF4
Current Density (A/cm2)
20
15
10
5
0
-1
0
1
Voltage (V)

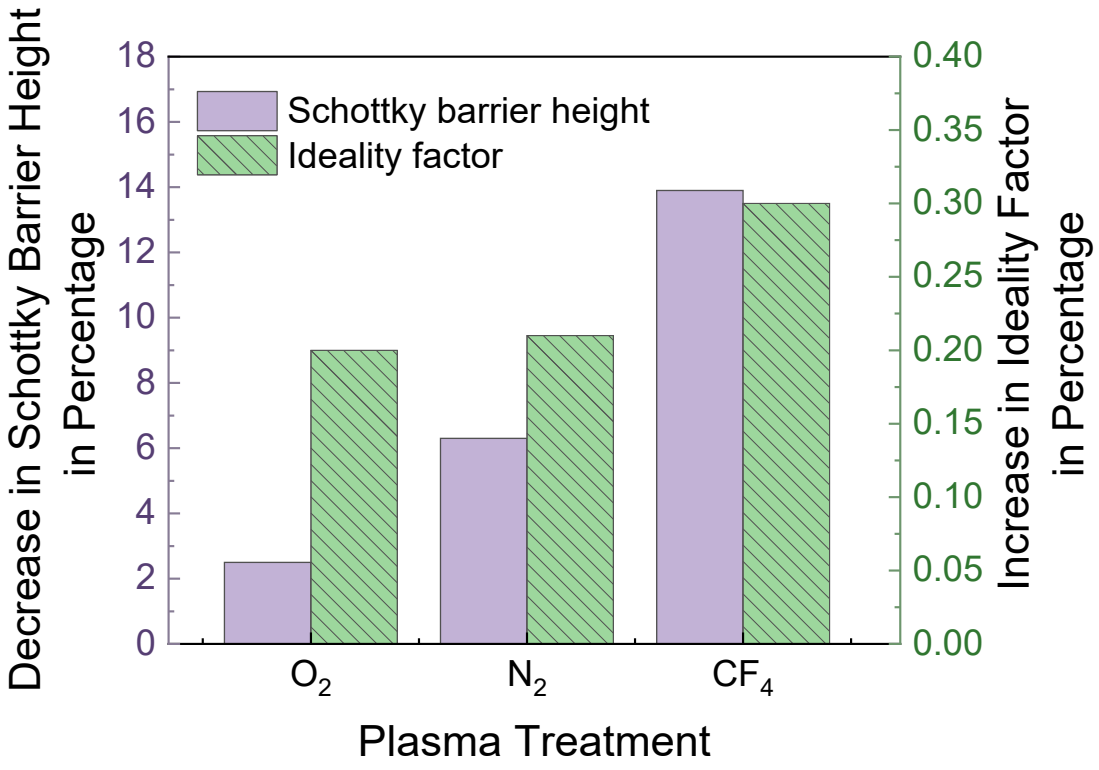
Decrease in Schottky Barrier Height in Percentage
Increase in Ideality Factor in Percentage
Schottky barrier height
Ideality factor
0
2
4
6
8
10
12
14
16
18
0.00
0.05
0.10
0.15
0.20
0.25
0.30
0.35
0.40
O2
N2
CF4
Plasma Treatment

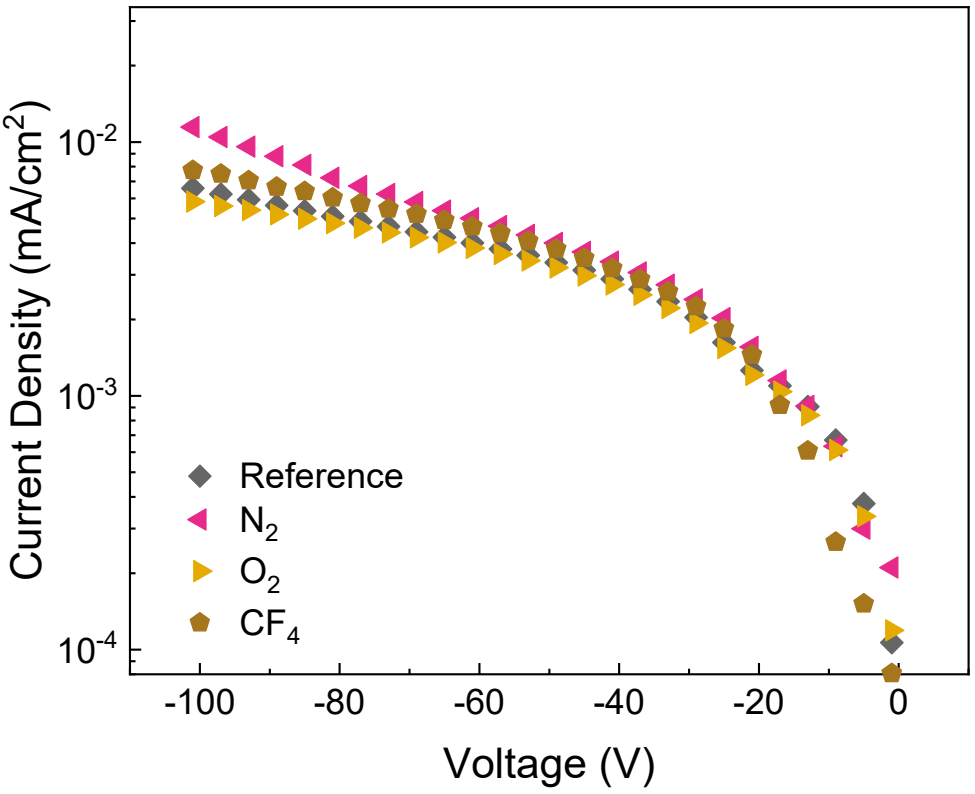
Current Density (mA/cm^2)
10^{-2}
10^{-3}
10^{-4}
Reference
N_2
O_2
CF_4
-100
-80
-60
-40
-20
0
Voltage (V)

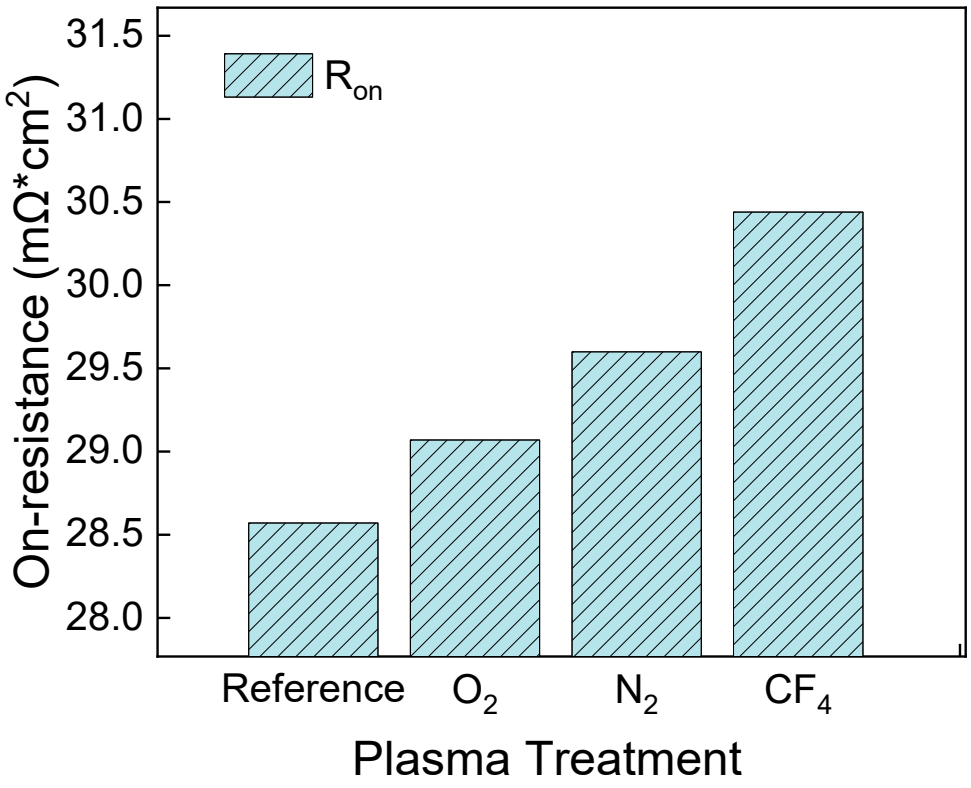
31.5
31.0
30.5
30.0
29.5
29.0
28.5
28.0
On-resistance (mΩ*cm2)
Ron
Reference
O2
N2
CF4
Plasma Treatment

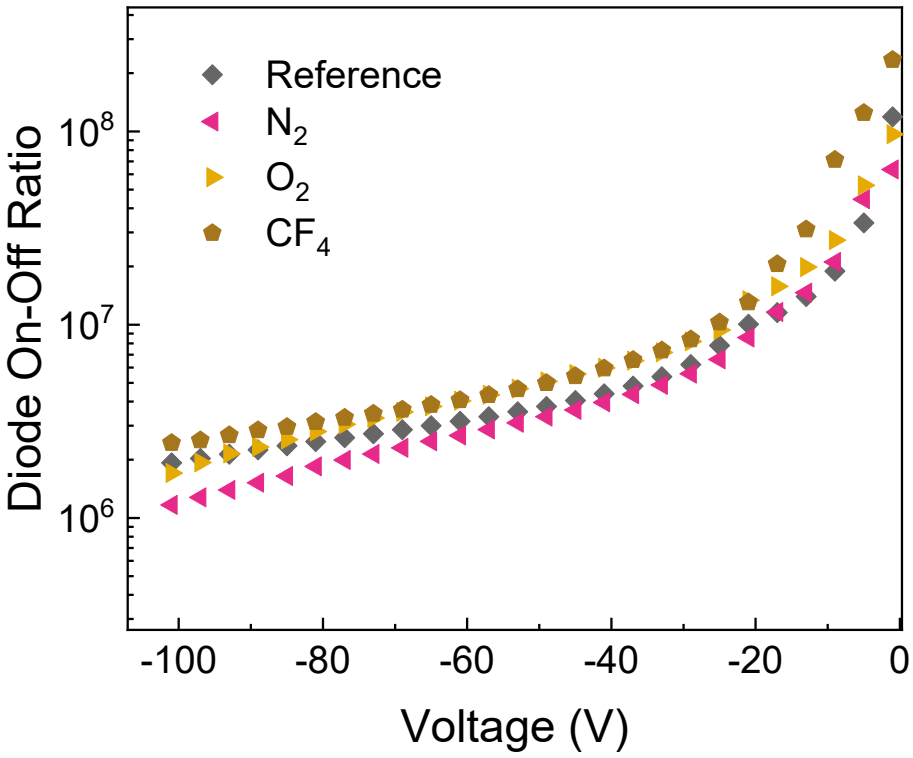
Reference
N2
O2
CF4
Diode On-Off Ratio
10^8
10^7
10^6
-100
-80
-60
-40
-20
0
Voltage (V)

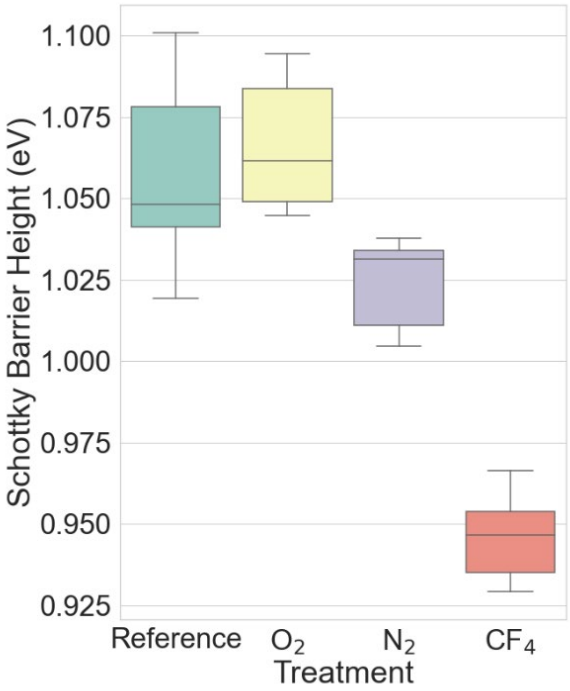
Schottky Barrier Height (eV)
1.100
1.075
1.050
1.025
1.000
0.975
0.950
0.925
Reference
O2
N2
CF4
Treatment

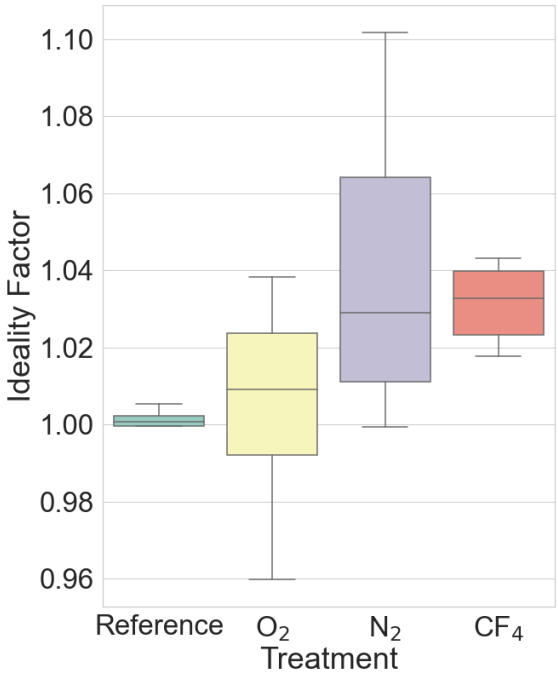
Ideality Factor
1.10
1.08
1.06
1.04
1.02
1.00
0.98
0.96
Reference
O2
N2
CF4
Treatment

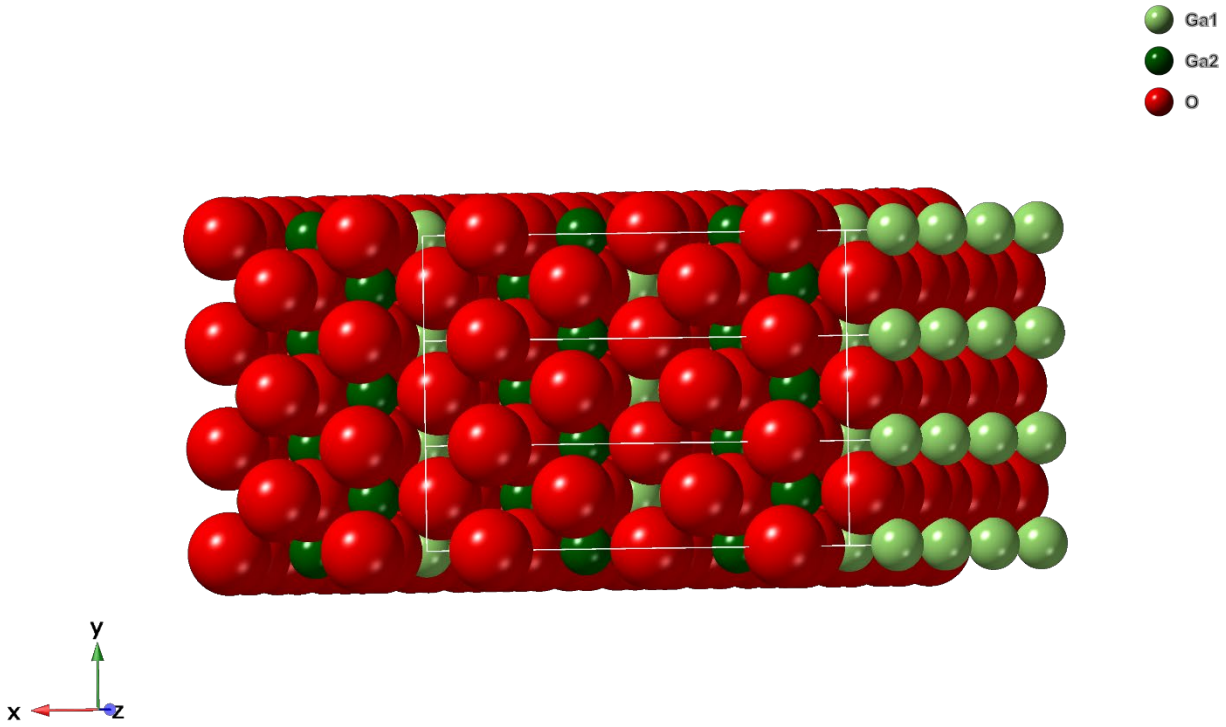
Ga1
Ga2
O
y
x
z